

Competition between diffusion and advection may mediate self-repair of wax microstructures on plant surfaces

Wilfried Konrad¹, Christoph Neinhuis¹, Anita Roth-Nebelsick²

¹ Technische Universität Dresden, Institut für Botanik, Germany

² State Museum of Natural History Stuttgart, Germany

Corresponding author: Wilfried Konrad, Technische Universität Dresden, Institut für Botanik, Zellescher Weg 20b, 01069 Dresden, Germany.

E-Mail: wilfried.konrad@tu-dresden.de

Abstract

Cuticles are extracellular membranes covering the primary aerial parts of vascular plants. They consist of a multifunctional polymeric material with embedded soluble components, called waxes and serve as the interface between plants and their atmospheric environment, first of all protecting them from desiccation. Waxes are produced within the epidermal cells, then transported to the leaf surface and finally integrated into the polymer or deposited upon the cuticle. Remarkably, damaged wax layers may become repaired within a few hours. Base on an earlier hypothesis we present a theoretical framework explaining how waxes are transported through the plant epidermis by a combination of advection and diffusion. This combination suggests also a self-regulating repair mechanism, based on the assumption that intact cuticles induce an antagonistic equilibrium between advection and diffusion: whenever a wax layer is damaged, the equilibrium is disturbed in favour of advection, starting a repair process, which is intrinsically coming to an end after the cuticle has gained its original thickness.

Keywords

Plant surface, self-repair mechanism, cuticle, diffusion, advection

1 Introduction

1.1 Biological background

Prior to the emergence and radiation of land plants in the early Silurian, most probably tracing back to the Ordovician, a new plant structure appeared that nowadays is called the cuticle. Although the systematic nature of the first organisms forming this new kind of extracellular



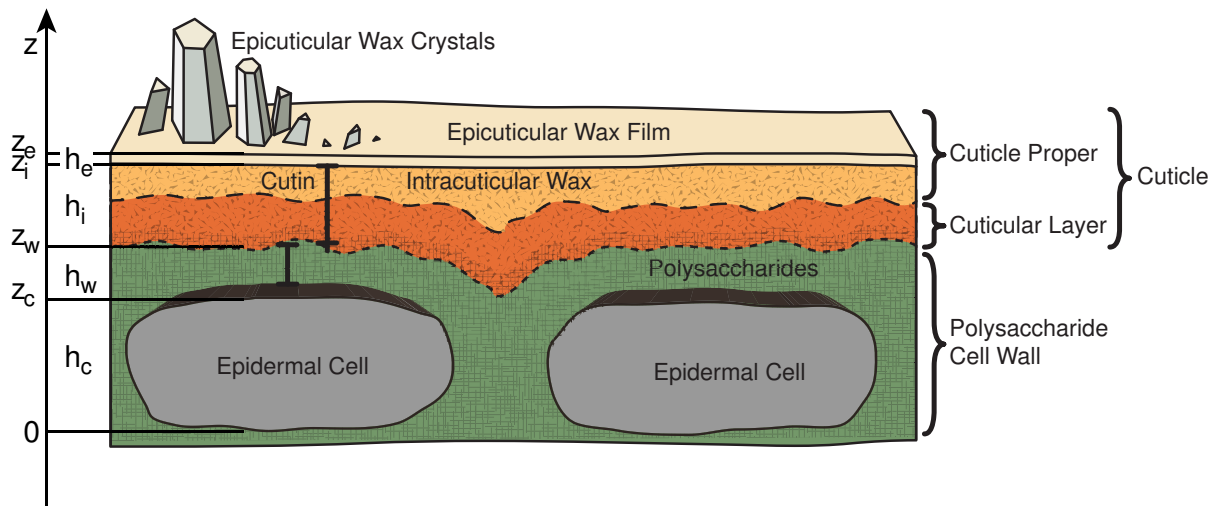


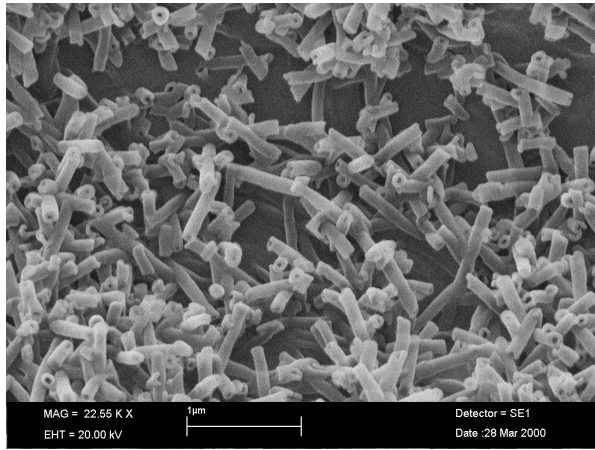
Figure 1: Plant cuticle structure. Schematic diagram highlighting the major structural features of the cuticle and underlying epidermal cell layer. h_e , h_i , h_w and h_c denote the thicknesses of the various layers, z_e , z_i , z_w and z_c the z -coordinates of their outer fringes. (Not drawn to scale, modified after [1]). For photographs of epicuticular waxes see Figure 2.

material remains controversial (they are often collectively called Nematophytes [2]), the cuticle proved to be one of the key innovations of plants to overcome the challenges of living on land, protecting them first and foremost from desiccation [3, 4]. The cuticle (see Figure 1) represents a thin extracellular membrane covering the primary aerial parts of vascular plants and many, if not all, bryophytes. It is a multifunctional polymeric material with embedded soluble components serving as the interface between plants and their atmospheric environment [5, 6]. During recent years, extensive research has contributed to the knowledge about structure, composition, biosynthesis, biotic and abiotic interactions, as well as functional aspects of the cuticle. But also the molecular and genetic background has made considerable progress summarized in detail by [7, 8, 9, 10, 11, 12, 13].

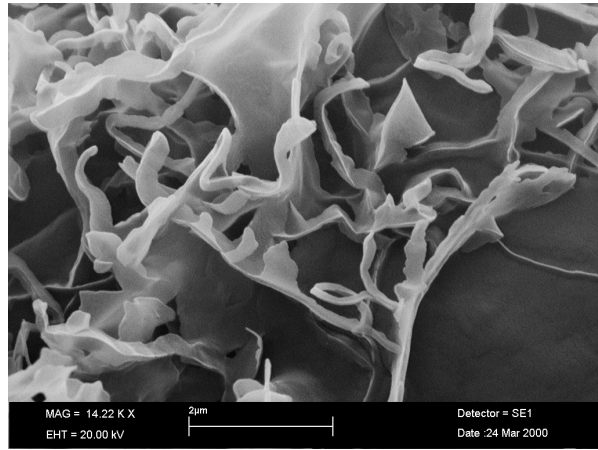
1.2 Chemical composition of the cuticle

The cuticle may be regarded as a natural composite comprising two major hydrophobic components: an insoluble polymer fraction composed of cutin and, in some species, cutan as well as soluble lipids of diverse chemistry, collectively called waxes. In addition, a certain amount of polysaccharides is present (overview in [14, 5]). The outer very thin region (usually less than 100 nm), called cuticle proper, contributes for 99 % of the barrier efficiency [4], while the region determining the thickness of up to 20 μm , is called the cuticle layer [15, 10]. Chemical composition and internal structure of the cuticle seems to show a high degree of variability during ontogeny and among different plant species and organs. Cutin basically is a biopolyester consisting of saturated C_{16} ω -hydroxy and unsaturated C_{18} hydroxyepoxy fatty acid monomers [16, 5, 12, 13] the ratio of which can be organ- as well as species-specific, and may change during ontogeny [17, 18, 19].

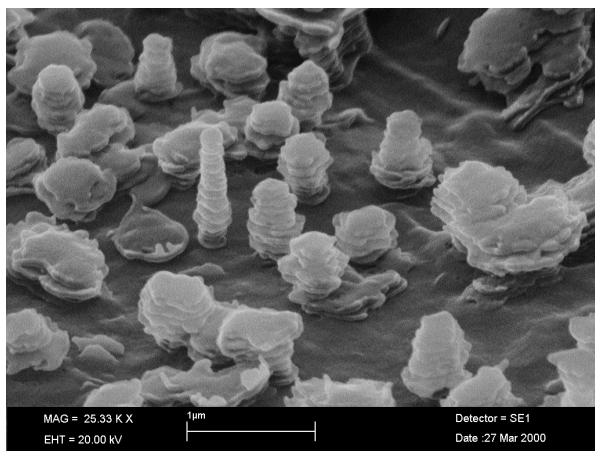
The polymer structure is found to be based on esters of primary hydroxyl groups of the fatty acid monomers forming a linear polyester, while the three-dimensional network is a result of branching combined with cross-linking between mid-chain groups and other constituents (e.g. [20, 21, 22]). Modelling the molecular structure of the polymer allowed calculating an average pore size of 0.3 nm – 0.5 nm [23, 24]. However, identifying the detailed three-dimensional structure of cutin still remains a challenging task [11].



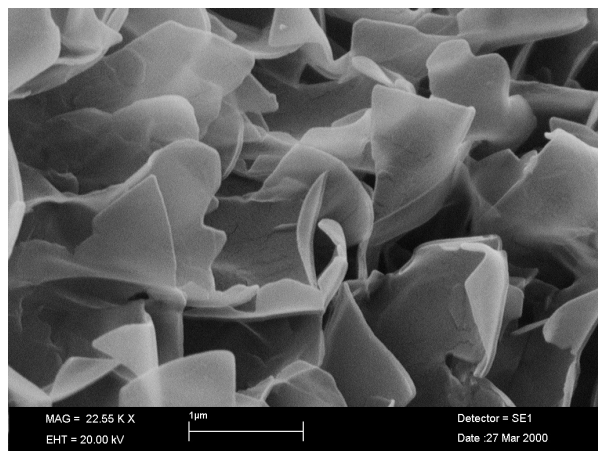
(a)



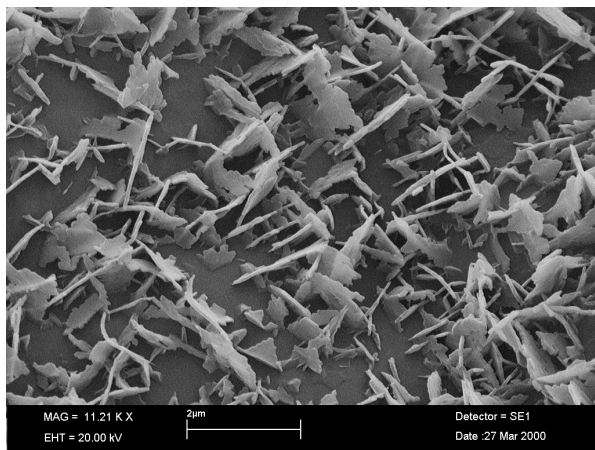
(b)



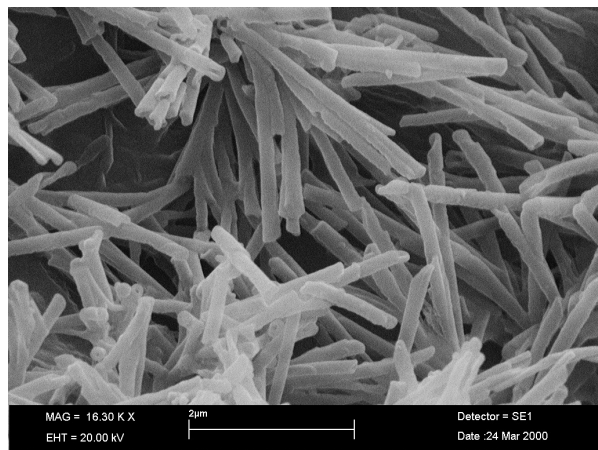
(c)



(d)



(e)



(f)

Figure 2: Scanning electron microscopic images of epicuticular waxes from plants. (a) Nonacosanol-based tubules (bar: 1 μm). (b) Irregular shaped wax crystals (bar: 2 μm). (c) Transversely ridged rodlets based on palmitone (bar: 1 μm). (d) Membraneous platelets (bar: 1 μm). (e) Irregularly shaped platelets (bar: 2 μm). (f) Tubules based on β -diketones (bar: 2 μm). Photographs: Institut für Botanik, TU Dresden

Cuticular waxes are either found within the cuticle determining water permeability or as a layer deposited upon the surface called epicuticular waxes (see Figure 2). Depending on the chemical composition epicuticular waxes are able to form complex three-dimensional crystalline structures, which may serve as valuable characters in plant systematics (e.g. [25, 26, 27]). All distinct wax crystals, however, emerge from an underlying wax film [28, 29, 30]. Intracuticular wax and epicuticular wax may differ in chemical composition as shown by [31] or [32]. Cuticular waxes represent mixtures comprising aliphatic and aromatic components, most of them with chain lengths ranging from C₂₀ to C₄₀ [14, 27, 33]. Depending on functional groups (-hydroxyl, -carboxyl, -keto) a broad spectrum of fatty acids, primary alcohols, aldehydes, β -diketones and secondary alcohols is detected [34, 35, 33]. Not uncommon, however, are aromatic compounds such as flavonoids or triterpenoids (e.g. [36, 37]). Cuticular wax composition again shows a huge variability, among plant species or different organs as well as during ontogeny [38, 39].

The apparent chemical diversity finds its expression also in a large variability in micro-morphology. Epicuticular wax crystals, however, often consist of a single predominating component or substance class resulting in a characteristic morphology. Such connections between chemistry and morphology are especially known for wax tubules and some wax platelets. While one type of tubules is based on secondary alcohols, predominantly 10-nonacosanol and its homologues [40, 41, 42, 43] while the second type is dominated by β -diketones such as hentriacontan-14,16-dione [44, 42]. Wax platelets are widespread among plants although differing in shape, chemical composition and distribution [45]. Besides aliphatic components such as primary alcohols (e.g. Poaceae, Fabaceae and the genus *Eucalyptus* [46, 47]).

The morphology of wax crystals is not necessarily depending on one dominating chemical compound or compound class only, but can also be determined by a minor component within a complex mixture as it was proven for transversely ridged rodlets [48]. While the chemical composition of cuticular waxes is hardly effected by environmental influences such as temperature and relative humidity the total amount of wax as well as crystal density, may be affected [49, 50, 51].

1.3 Crystallinity of cuticular waxes

Whereas intra-cuticular waxes may be either amorphous or crystalline, epicuticular waxes (Figure 2) are assumed to be of crystalline nature [47, 52, 51]. De Bary [53], in his pioneering work applied the term 'crystalloid' to epicuticular waxes. Nowadays, based on a number of investigations using X-ray powder diffraction, electron diffraction, and nuclear magnetic resonance (NMR) spectroscopy the crystalline nature of various wax types is broadly accepted [42, 43, 52, 54].

The crystal nature of epicuticular waxes implies self-assembly as the driving force for the formation of such structures. This has been proven by dissolving in and recrystallizing waxes from organic solvents revealing morphologically similar structures as compared to the plant surface [55, 41, 40, 48, 42, 56, 47, 52, 57]. To allow self-assembly of complex three-dimensional structures, the individual molecules must be mobile within a suitable matrix or solvent in which they are free to find an energetically favourable position, which also includes phase separation of different components or component classes found in wax mixtures. Re-crystallisation of extracted waxes from a solution is considerably influenced by temperature, chemical nature of the solvent and the underlying substrate resulting in a large structural variability [47, 51].

The most intriguing problem, however, was the movement of wax molecules onto the surface, as they have to move from inside the cell through a hydrophilic cell wall and the hydrophobic cuticle and finally onto the ridges and edges of the growing crystals. Several hypotheses have

been published from ectodesmata to the involvement of transport proteins [58, 59, 60]. One obvious hypothesis is the existence of some kind of channels or pathways but no evidence of trans-cuticular structures that could serve as pathways for wax molecules have yet been found in the plant cuticle by SEM, TEM or AFM investigations [61, 56].

Neinhuis, Koch et al. [62] proposed a co-transport of wax components with water that constantly is lost via the cuticle, although in very small amounts. The hypothesis postulates a transport of waxes similar to water vapour distillation, i.e. wax molecules are much more mobile in the polymer phase in the presence of water as compared to a situation without water a process later adopted also by [63] for cuticle formation. Assuming such a process is appealing since no pathways, carrier molecules or sensors are needed. Since cuticular waxes are the main permeability barriers, the transport to the outside slows down while more wax is deposited on the surface, so it is self-regulating. In addition it easily explains the intriguing phenomenon of wax regeneration. Since removal of epicuticular wax also partly removes the water barrier, more wax is able to move through the cuticle in this particular spot and builds up a new layer without affecting neighbouring area. Atomic Force Microscopy *in situ* demonstrated the rather quick reassembly of new wax layers after their removal under environmental conditions *in vivo*. AFM time-series pictured the formation of mono- and bimolecular wax films and the growth of three-dimensional platelets, either directly on the cuticle or on already existing wax layers within minutes [30, 56].

In this paper we will present a model providing support for the hypothesis of a co-transport of waxes together with water. The model is based on the scenario of cuticle repair outlined above (cf. Figure 1):

- Intact cuticles are very efficient barriers against transpiration of water from the plant interior. Hence, if the wax layer is degraded, evaporation from this zone increases, generating a current of liquid water from the plant interior.
- This water current transports the wax molecules from the epidermal cells (where they are presumably produced) towards the outer fringe of the cuticle. There the water evaporates. Being much heavier than the water molecules, the wax molecules do not evaporate, they rather form wax crystals rebuilding hereby the damaged cuticle layer by layer.
- As this repair process proceeds, both evaporation and the evaporation driven water current decrease and smaller amounts of wax molecules are transported to the damaged cuticle. Finally, the cuticle attains its original thickness and the repair process comes to a halt.

2 The model

2.1 Assumptions

In order to translate the above scenario into mathematical terms we make the following assumptions:

- We employ the porous medium approximation, allowing to restrict the mathematics to one dimension (the z -direction in Figure 1). Thus, all variables depend only on z .
- The properties of the biological structures along the z -axis are supposed to be (approximately) constant within each of the four different layers depicted in Figure 1.
- We assume stationary conditions, that is, none of the transport processes involved depends explicitly on time.

- We take into consideration two transport mechanisms for the wax molecules: Diffusion between and advection by the (liquid) water molecules.

2.2 Derivation of the transport equation

The (one-dimensional) flux of wax molecules of concentration $c(z)$ is given by the expression (see e.g. [64, 65])

$$j = -S \frac{dc}{dz} + cJ \quad . \quad (1)$$

The first term on the right hand side describes diffusion, the second term advection with $J(z)$ denoting the flux of (liquid) water. $S = Dn/\tau$ denotes the diffusion coefficient in a porous medium, n and τ are porosity and tortuosity of that medium, respectively, and D is the diffusion coefficient in bulk liquid.

Stationarity and one-dimensional approach effectuate that the continuity equation $\partial c/\partial t = -\text{div } \vec{j} + q$ for the wax molecules reduces to

$$0 = -\frac{dj}{dz} + q \quad . \quad (2)$$

q denotes a source (or sink) term, describing the insertion of wax molecules into (or their removal from) the cell water. We assume that the wax molecules originate only within the epidermal cells. This implies $q = 0$ outside the interval $0 < z < z_c$. Within this interval we set

$$q = \xi [c_t - c(z)] \quad (3)$$

where c_t denotes a threshold concentration of the wax molecules and ξ is a rate constant. Depending on whether $c_t > c(z)$ or $c_t < c(z)$ is realised, q acts as source term (i.e. producing wax molecules, $q > 0$) in the first case and as sink term (removing wax molecules, $q < 0$) in the second case. Obviously, the maximum production rate of wax molecules amounts to $q_{max} = \xi c_t$.

Insertion of expressions (1) and (3) into the continuity equation (2) generates the linear second order differential equation

$$-S \frac{d^2c}{dz^2} + \frac{d(cJ)}{dz} = \begin{cases} \xi (c_t - c) & \text{if } 0 < z < z_c \\ 0 & \text{if } z_c < z < z_e \end{cases} \quad (4a)$$

$$(4b)$$

As noted above, we assume that the properties of the plant tissue — represented by the variables S , n and τ — are approximately constant within each of the four different layers of Figure 1. They may, however, vary from one layer to the next. This implies that equation (4b) has to be solved separately for the three layers between $z = z_c$ and $z = z_e$.

In a second step, these three solution plus the solution of (4a) are pierced together such that wax concentration $c(z)$ and wax flux $j(z)$ become continuous functions at the “inner” layer margins z_c , z_w and z_i . This is achieved by assigning appropriate values to six of the eight integration constants which emerge from the solution of (4a) and (4b).

2.3 Solution of the water flux equation

Before we can tackle equation (4) we have to determine the still unknown water flux $J(z)$ between the epidermal cell and the outer fringe of the cuticle.

Because the plant tissues we deal with can be treated as porous media and because the fluid velocities inside these are low it is reasonable to describe $J(z)$ by means of Darcy’s Law (see e.g. [64, 65, 66]). In one dimension it reads

$$J = -K \frac{d\psi}{dz} \quad . \quad (5)$$

$K(z)$, the hydraulic conductivity, contains information about the flowing liquid (which is in our case water loaded with wax crystals) and the conductivity of the structures through which the liquid flows. Similarly as before, we assume that $K(z)$ is constant within each of the four tissue layers but may vary from layer to layer.

$\psi(z)$ denotes the water potential whose gradient $d\psi/dz$ is the driving force of the water current. The water potential of atmospheric water vapour depends on temperature T and relative humidity w_{rel} (see e.g. [66]) according to

$$\psi_{wv} = \frac{RT}{V_w \rho_w g} \log w_{rel} \quad . \quad (6)$$

R , g , ρ_w and V_w denote the gas constant, the gravitational acceleration, and the density and molar volume of liquid(!) water, respectively.

The water flux equation is derived from the continuity equation which reduces due to our assumptions to

$$0 = \frac{dJ}{dz} \quad . \quad (7)$$

Insertion of (5) — while keeping in mind the assumption that $K(z)$ is constant within each layer — yields the differential equation

$$0 = \frac{d^2\psi}{dz^2} \quad (8)$$

which has to be solved separately for each layer. Each of the four solutions of equation (8) contains two arbitrary constants. These are determined from

- the condition of continuity for the water potential $\psi(z)$ and the water flux $J(z)$ at the layer margins at z_c , z_w and z_i and from
- two boundary conditions for $\psi(z)$: We require $\psi(0) = \psi_{leaf}$ and $\psi(z_e) = \psi_{wv}$ with ψ_{wv} as given in (6).

Application of this procedure is straightforward. It results, however, in lengthy expressions for $\psi(z)$; since we do not need them in what follows we omit them here. It turns out that $J(z)$ is independent of z (which was to be expected from the physics of the situation: no water sources or sinks are present). It reads

$$J = \frac{\psi_0 - \psi_{wv}}{\frac{h_c}{K_c} + \frac{h_w}{K_w} + \frac{h_i}{K_i} + \frac{h}{K_e}} \quad . \quad (9)$$

h_e , h_i , h_w and h_c denote the thicknesses of the various layers, as indicated in Figure 1. $J > 0$ indicates a water flux towards positive z -values, i.e. towards the plant surface. In what follows, h_e denotes the thickness of the intact epicuticular wax film while h denotes its actual thickness during any stage of the repair process (thus, $0 \leq h \leq h_e$).

Notice that J depends roughly reciprocally on the thickness h of the epicuticular wax film. Thus, the water flux represented by expression (9) decreases while the repair process proceeds and the wax layer regains its original thickness.

2.4 Formal solution of the transport equation

Having derived the water flux J , we return to the transport equation (4). Considering that S , J and ξ can be treated as constants within a given layer, the solutions of (4) are

$$c(z) = \begin{cases} c_t + a_c \exp\left(\frac{zJ - z\sqrt{J^2 + 4\xi S_c}}{2S_c}\right) + b_c \exp\left(\frac{zJ + z\sqrt{J^2 + 4\xi S_c}}{2S_c}\right) \\ a_w + b_w \exp\left(\frac{zJ}{S_w}\right) & \text{if } z_c < z < z_w \\ a_i + b_i \exp\left(\frac{zJ}{S_i}\right) & \text{if } z_w < z < z_i \\ a_e + b_e \exp\left(\frac{zJ}{S_e}\right) & \text{if } z_i < z < z_e \end{cases} \quad (10)$$

The first line applies within the epidermal cell (i.e. for $0 < z < z_c$). a_c , b_c , a_w , b_w , a_i , b_i , a_e and b_e are arbitrary constants. The flux of the wax molecules is obtained by inserting (10) into (1). One finds

$$j(z) = \begin{cases} c_t J + \frac{a_c}{2} (J + \sqrt{J^2 + 4\xi S_c}) \exp\left(\frac{zJ - z\sqrt{J^2 + 4\xi S_c}}{2S_c}\right) \\ \quad + \frac{b_c}{2} (J - \sqrt{J^2 + 4\xi S_c}) \exp\left(\frac{zJ + z\sqrt{J^2 + 4\xi S_c}}{2S_c}\right) \\ a_w J & \text{if } z_c < z < z_w \\ a_i J & \text{if } z_w < z < z_i \\ a_e J & \text{if } z_i < z < z_e \end{cases} \quad (11)$$

As above, the first line applies within the epidermal cell (i.e. for $0 < z < z_c$). The water flux J is given by (9).

2.5 Boundary conditions for the wax transport equation

As pointed out in section 2.2 equation (4) has to be solved separately for each of the four different layers depicted in Figure 1.1.. This approach produces eight arbitrary constants which have to be determined from the following eight conditions.

- Six “inner” boundary conditions: they ensure that the concentrations $c(z)$ and the fluxes $j(z)$ are continuous functions at the layer margins at z_c , z_w and z_i (cf. Figure 1).
- The saturation concentration c_s represents an upper limit for the concentration of wax molecules in liquid water. Liquid water flowing through the epicuticular wax film is in contact with already crystallised wax molecules and will thus be saturated with wax. Therefore, at $z = z_e$, the outer fringe of the cuticle, $c(z)$ should attain the value

$$c(z_e) = c_s \quad (12)$$

- Diffusion allows the wax molecules to move upstream, i.e. against the flow direction of the water flux J whereas (pure) advection does not offer this possibility. Thus, wax molecules produced within the epidermal cell sufficiently close to $z = 0$ may diffuse into the region $z < 0$ whatever value the water flux J has. However, if diffusion is excluded and (pure) advection prevails this should not happen. Hence, the requirement

$$\lim_{S_c \rightarrow 0} j|_{z=0} = 0 \quad (13)$$

is appropriate. We prefer (13) to the obvious condition $j|_{z=0} = 0$ which prohibits wax flux across the $z = 0$ -cross section absolutely because most biological materials could not guarantee that. Thus, the choice (13) is probably closer to reality than $j|_{z=0} = 0$.

2.6 Specific solution of the transport equation

The application of the boundary conditions of section 2.5 to the formal solutions (10) and (11) is straightforward leads, however, to lengthy expressions for the wax concentration $c(z)$. Since we need in what follows merely the wax flux we present only $j(z)$:

$$j(z) = \begin{cases} \left. \begin{aligned} & c_t J - \frac{c_t}{2} \left(J + \sqrt{J^2 + 4\xi S_c} \right) e^{\frac{zJ - \sqrt{J^2 + 4\xi S_c}}{2S_c}} \\ & + \frac{c_t N_-}{2N_+} \left(J - \sqrt{J^2 + 4\xi S_c} \right) e^{\frac{(J + \sqrt{J^2 + 4\xi S_c})(z - z_c)}{2S_c}} e^{\frac{z_c J - z_c \sqrt{J^2 + 4\xi S_c}}{2S_c}} \\ & + \frac{c_s J}{2N_+} \left(J - \sqrt{J^2 + 4\xi S_c} \right) e^{\left(\frac{z_i J}{S_e} + \frac{z_w J}{S_i} + \frac{z_c J}{S_w} \right)} e^{\frac{(J + \sqrt{J^2 + 4\xi S_c})(z - z_c)}{2S_c}} \end{aligned} \right\} & \text{if } 0 < z < z_c \end{cases} \quad (14a)$$

$$j(z) = \begin{cases} \left. \begin{aligned} & \frac{c_t J}{N_+} \left(J + \sqrt{J^2 + 4\xi S_c} \right) e^{\left(\frac{(z_i + h)J}{S_e} + \frac{z_i J}{S_i} + \frac{z_w J}{S_w} \right)} \\ & - 2 \frac{c_t J}{N_+} \sqrt{J^2 + 4\xi S_c} e^{\left(\frac{z_c J - z_c \sqrt{J^2 + 4\xi S_c}}{2S_c} \right)} e^{\left(\frac{(z_i + h)J}{S_e} + \frac{z_i J}{S_i} + \frac{z_w J}{S_w} \right)} \\ & + \frac{c_s J}{N_+} \left(J - \sqrt{J^2 + 4\xi S_c} \right) e^{\left(\frac{z_i J}{S_e} + \frac{z_w J}{S_i} + \frac{z_c J}{S_w} \right)} \end{aligned} \right\} & \text{if } z_c < z < z_e \end{cases} \quad (14b)$$

with

$$N_{\pm} := \left(J \pm \sqrt{J^2 + 4\xi S_c} \right) e^{\left(\frac{(z_i + h)J}{S_e} + \frac{z_i J}{S_i} + \frac{z_w J}{S_w} \right)} + \left(J \mp \sqrt{J^2 + 4\xi S_c} \right) e^{\left(\frac{z_i J}{S_e} + \frac{z_w J}{S_i} + \frac{z_c J}{S_w} \right)} .$$

The water flux J is given by (9). Notice that the wax flux j is a function of z merely within the epidermal cell, that is for $0 < z < z_c$; it is constant for $z_c < z < z_e$. Since neither wax sources nor sinks are present in the latter interval, this behaviour is to be expected.

2.7 Self-regulation of the repair process

The transport equation (4) and its solution (14) (resp. (10)) with (9) encompass both advection and diffusion as transport mechanisms. In order to understand the repair scenario in terms of physics it is instructive to consider the limits of $j(z)$ if either of these mechanisms is disregarded. We give only the expressions valid within $z_c < z < z_e$; those within $0 < z < z_c$ produce very lengthy results.

$$\lim_{S_c \rightarrow 0} j(z) = c_t J \left[1 - e^{\left(-\frac{z_c \xi}{J} \right)} \right] \quad (15)$$

$$\lim_{J \rightarrow 0} j(z) = \frac{c_t \left[1 - 2 e^{\left(-z_c \sqrt{\frac{\xi}{S_c}} \right)} \right] - c_s}{\frac{h_w}{S_w} + \frac{h_i}{S_i} + \frac{h}{S_e} + \frac{h_w}{S_w} + \frac{1}{\xi S_c}} \quad (16)$$

The first expression is positive because of the minus sign in the argument of the exponential function and because all variables in the expression ought to be positive, in order to be meaningful; thus, as long as the liquid water flows towards the cuticle, advective wax flow is also directed towards the cuticle. By similar reasoning, the second expression is always negative (c_s is the saturation concentration, this implies $c_s \geq c_t$). Hence, pure diffusive transport is directed towards the leaf interior, away from the cuticle.

It seems likely that this competition between diffusive and advective flow forms the basis of the self-regulating repair process:

1. For an intact cuticle the antagonistic transport efforts of diffusion and advection just cancel each other, no wax molecules are moved.
2. If the cuticle is degraded this fine tuned equilibrium is violated in favour of advection: the water flux J increases according to (9) (cf. also Figure 1) while the concentration gradient which drives diffusion remains nearly unchanged.
3. As a consequence of this imbalance, a current of wax molecules towards the cuticle arises, they are brought to and incorporated into the damaged cuticle.
4. This restoration process increases the cuticle thickness which results in a decrease of the water flux, quantified by expression (9), and thus a decrease of the wax flux, according to expression (14b).
5. Finally, the initial cuticle size is restored and the balance between diffusion and advection is reconstituted.

In this picture, the self-regulation of the wax transport from epidermal cell to cuticle emerges only if both advection and diffusion are included in the transport equations. If they are reduced to pure advective or pure diffusive transport, the effect of self-regulation disappears.

3 Results

3.1 Concentrations and fluxes

Figure 3 displays the wax concentration $c(z)$ and the wax flux $j(z)$ along the pathway of wax molecules between epidermal cell and epicuticular wax film (cf. Figure 1) and the wax production rate $q = \xi [c_t - c(z)]$ within the epidermal cells. Numerical values are as given in Table 1.

Subfigure c shows the (net) wax flux $j(z)$. It is the sum of the diffusive component (represented by the first term in expression (1)) and of the advective component (the second term in (1)). These two are displayed in subfigure d; the upper three curves represent advective components, cJ , the lower three curves depict the diffusional parts, $-S dc/dz$. Positive fluxes are directed towards the cuticle, negative fluxes point to the leaf interior. Blue curves are related to a damaged cuticle (the outer fringe is located at $z = z_i$), green curves represent an intact cuticle (the outer fringe is at $z = z_e$), and red curves represent the fictitious case of an epicuticular wax film which is twice as thick as it ought to be.

Comparison between the blue and green curves allows to visualise the repair scenario:

- As long as the cuticle is undamaged, the green curves terminate at $z = z_e$, and the green curves representing advection and diffusion (subfigure d) have for all points with $z > z_w$ the same distance to the z -axis, thus adding up to a vanishing net flux (green curve in subfigure c).

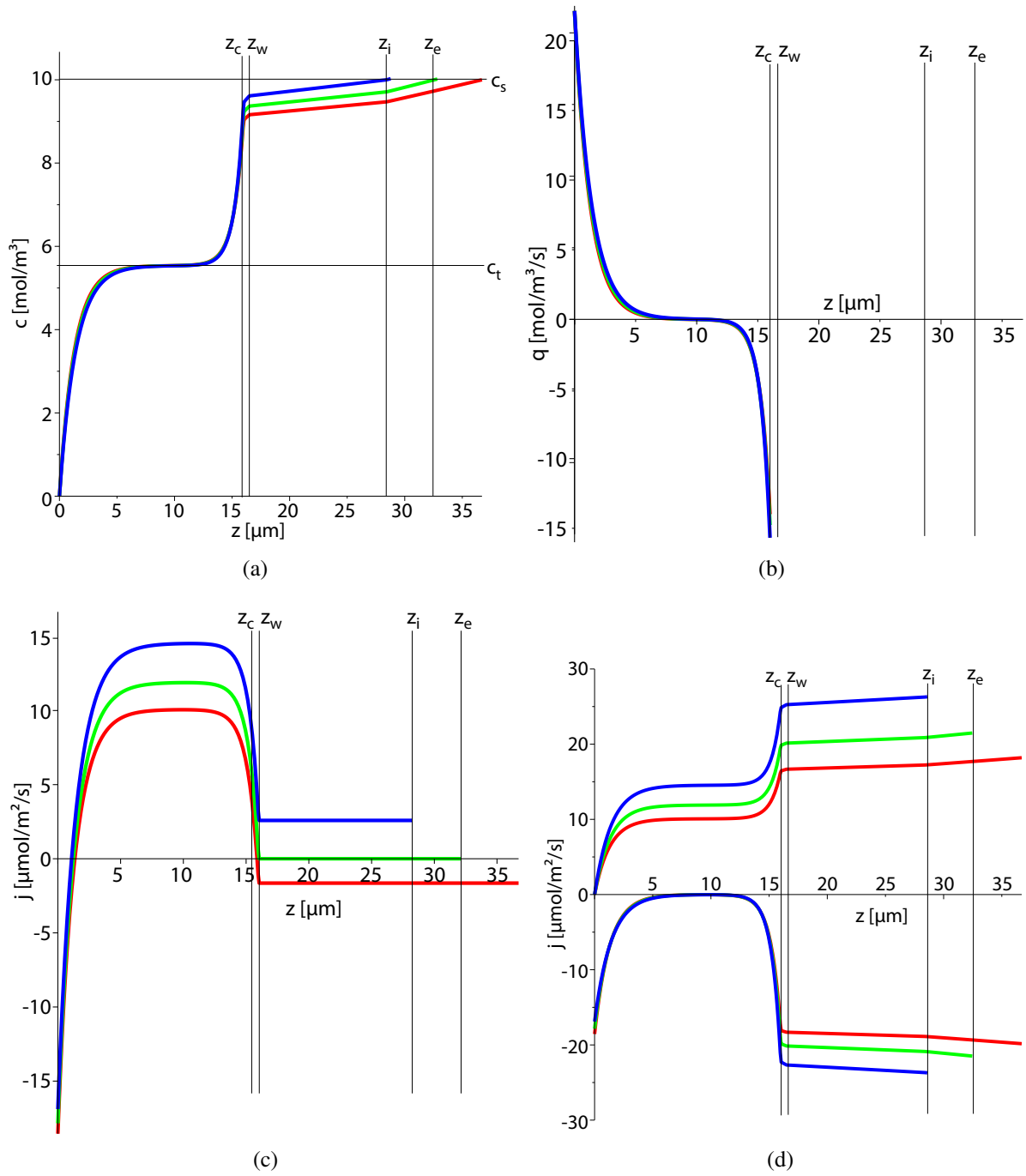


Figure 3: Wax concentration (a) and wax fluxes (c,d) along the pathway of wax molecules between epidermal cell and epicuticular wax film (cf. Figure 1) according to expression (14).

The (net) wax flux $j(z)$ in subfigure c is the sum of the diffusive component (lower three curves in subfigure d) and of the advective component (upper three curves in subfigure d). Positive fluxes are directed towards the cuticle, negative fluxes point to the leaf interior. (For detailed explanation see text.)

Vertical lines delineate the tissue layers defined in Figure 1; the horizontal lines in subfigure (a) denoted c_s and c_t mark the saturation and the threshold wax concentrations introduced in section 2.2.

Subfigure (b) depicts the wax insertion (or removal) rate $q = \xi [c_t - c(z)]$ within the epidermal cells. Positive values indicate insertion, negative values indicate removal of wax molecules. Notice that the graph depicts three nearly identical curves.

Numerical values are as in Table 1

- When the cuticle is damaged the repair process begins. This is illustrated by the blue curves which terminate at $z = z_i$: the absolute values of both advection and diffusion flux have increased, compared to the intact cuticle (see subfigure d), but now results a net flux towards the cuticle (see subfigure c).
- During the cuticle regrowth all blue curves “migrate” towards the green curves, that is, the absolute values of advection and diffusion flux decrease and converge slowly until they have merged with the green curves; then the net flux ceases and the repair process is completed.

Notice, that the model predicts also what happens to (fictitious) protrusions of height $h > h_e$, extending from the epicuticular wax film: This case is represented by the red curves. The one representing the net flux (subfigure c) runs for $z > z_w$ below the z -axis, indicating a negative net flux directed towards the plant interior; this means that the protrusions are dissolved and transported to the leaf interior. This process stops when the cuticle has been eroded to thickness h_e and the red curve has migrated to and merged with the green curve.

Comparison of subfigures b and c of Figure 3 illustrates the continuity equation (2) which states that the gradient of the net wax flux equals the injection (or removal) of wax molecules: The region $0 < z \lesssim 8 \mu\text{m}$ acts as a wax source (indicated by $q > 0$). Wax molecules that are generated in the region $z \lesssim 2 \mu\text{m}$ flow towards the plant interior (indicated by $j < 0$), those produced in the interval $2 \mu\text{m} \lesssim z \lesssim 8 \mu\text{m}$ flow a short distance towards the cuticle (indicated by $j > 0$). In the case of an intact cuticle (green curves), all of them are removed from the cell liquid in the region $8 \mu\text{m} \lesssim z < z_c$ which acts as wax sink ($q < 0$). If the cuticle is damaged (blue curves), however, a certain fraction of the injected wax molecules reaches and repairs the cuticle.

3.2 Restoration of the wax layer as a function of time

Provided the restoration proceeds slowly, compared to the travel time τ of a wax molecule between epidermal cell and epicuticular wax layer, the results of section 2.6 can be exploited to derive the temporal development of the wax layer repair, although they have been derived under the assumption of stationarity. The values given in Table 1 imply $J \approx 2.17 \mu\text{m/s}$ and thus $\tau = z_e/J \approx 15 \text{ s}$. Hence, if the repair process last perhaps one hour, this approach is certainly justified.

We assume that the epicuticular wax layer of thickness h_e has been eroded completely before the restoration process begins. That is, at the starting point of the restoration the outer fringe of the cuticle is located at $z = z_i$, equivalent to $h = 0$ (h denotes the actual thickness of the wax layer, h_e its thickness when it is intact, cf. Figure 1).

The water brought there by the water flux J evaporates from the eroded area, leaving behind the much heavier wax molecules that came by the wax flux j . The wax molecules organise themselves as crystals, thus restoring the wax layer until it reaches its original thickness h_e when the wax flux j breaks down.

If V_{wax} denotes the molar volume of the wax molecules, the thickness h of the wax layer regrows with the velocity

$$\frac{dh}{dt} = V_{wax} j(h) \quad . \quad (17)$$

In view of the structure of expressions (14b) and (9), this is a non-linear ordinary differential equation for $h(t)$.

The obvious solution strategy is to rearrange it and to perform the following integration:

$$\frac{1}{V_{wax}} \int_0^h \frac{d\tilde{h}}{j(\tilde{h})} = \int_0^t d\tilde{t} = t \quad . \quad (18)$$

Unfortunately, this straightforward approach fails due to the structure of the integrand $1/j(h)$. Instead, we content ourselves with an approximation and proceed as follows.

We know already h_e , the value of h where j vanishes; in terms of Figure 1 it is the outer margin of the intact leaf. Thus, we can expand j in a Taylor series with respect to h around h_e up to the first order, obtaining the approximation

$$j = j_0 + j_1 (h - h_e) \quad . \quad (19)$$

j_0 and j_1 are the expansion coefficients

$$j_0 := j|_{h=h_e} = 0 \quad (20)$$

$$j_1 := (\partial j / \partial h)|_{h=h_e} \quad (21)$$

Insertion of (19) through (21) into (18) yields

$$\frac{1}{j_1 V_{wax}} \int_0^h \frac{d\tilde{h}}{\tilde{h} - h_e} = \frac{1}{j_1 V_{wax}} \log \left[\frac{h_e - h}{h_e} \right] = t \quad , \quad (22)$$

and, after solving for h ,

$$h(t) = h_e \left[1 - e^{(j_1 V_{wax} t)} \right] \quad , \quad (23)$$

with j_1 as given in (21). According to this expression, the outer margin $h(t)$ of the wax crystal layer approaches its original thickness h_e asymptotically, that is, the repair process lasts — in principle — infinitely long; the time which is necessary to rebuild for instance 95 % of the layer is, however, finite and amounts to the value

$$t_{95} := \frac{\ln(20)}{-j_1 V_{wax}} \approx \frac{2.99}{-j_1 V_{wax}} \quad . \quad (24)$$

Figure 4 illustrates the result (23) for two different cases:

- In subfigure a, temperature is kept constant and the relative atmospheric humidity w_{rel} adopts three different values. The time spans t_{95} increase with increasing w_{rel} : this is to be expected because the water potential difference $|\psi_0 - \psi_{wv}|$ which is the driving force of evaporation decreases if w_{rel} is increased, according to (6). Accordingly, the wax supply for restoration decelerates.
- In subfigure b, relative atmospheric humidity is kept constant and temperature is varied ($T = 10^\circ\text{C}, 20^\circ\text{C}, 30^\circ\text{C}$). The related curves are nearly indistinguishable. This can be understood qualitatively: according to expressions (6) and (9), the water flux J is proportional to T . On the other hand, it is well-known (see e.g. [66, 67]) that the diffusional constants S_n are proportional to $T^{1.8}$ which implies a weak temperature dependence proportional to $T^{0.8}$ in the exponential terms of (14). Additionally, the relative differences within the two families of curves amount to 20 % if w_{rel} is varied, compared to 3.3 % if T is varied.

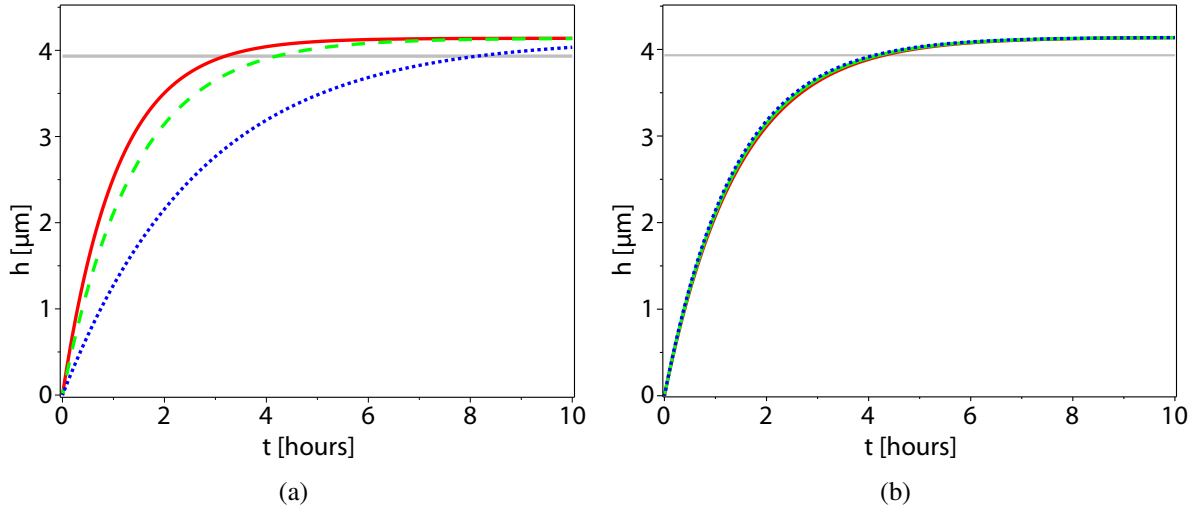


Figure 4: Growth of the wax layer with time according to expression (23). The intersections with the grey, horizontal line indicate the time it takes to rebuild the wax layer to 95 % of its original thickness of $h_e = 4.14 \mu\text{m}$.

(a) Temperature is kept constant at $T = 293 \text{ K} = 20^\circ\text{C}$ while the relative atmospheric humidity w_{rel} and the threshold concentration c_t of wax molecules in epidermal cell (see (25)) assume the values $(w_{rel}, c_t) = (0.8, 7.78 \text{ mol/m}^3)$ (blue, dotted line), $(w_{rel}, c_t) = (0.6, 5.53 \text{ mol/m}^3)$ (green, broken line) and $(w_{rel}, c_t) = (0.4, 3.48 \text{ mol/m}^3)$ (red, continuous line). The related time spans are $t_{95} = 8.13 \text{ h}$ (blue line), $t_{95} = 4.20 \text{ h}$ (green line) and $t_{95} = 3.19 \text{ h}$ (red line).

(b) $w_{rel} = 0.6$ is kept constant, T and c_t assume the values $(T, c_t) = (30^\circ\text{C}, 5.65 \text{ mol/m}^3)$ (blue line), $(T, c_t) = (20^\circ\text{C}, 5.53 \text{ mol/m}^3)$ (green line) and $(T, c_t) = (10^\circ\text{C}, 5.42 \text{ mol/m}^3)$ (red line). The three curves are nearly indistinguishable; their common t_{95} time amounts to $t_{95} = 4.20 \text{ h}$.

Other numerical values are as in Table 1. t_{95} is defined in (25)

3.3 Derivation of input data

To our knowledge, the literature does not provide a complete and consistent data set for all the parameters (cf. Table 1) that are necessary to check the feasibility of the model outlined above. Thus, instead of verifying the model in a strict sense we rather present a few illustrative results, displayed in Figures 3 and 4.

The missing data concerns the hydraulic conductivities K_n ($n = w, i, e$) (and thus, according to (9), the water flux J), the diffusion constant S_c , the saturation concentration c_s , and the values of the rate constant ξ and the threshold concentration c_t (the product of the latter two, $q_{max} = \xi c_t$, quantifies the maximum wax production rate in the epidermal cells).

- The threshold concentration c_t can be eliminated as an unknown quantity as follows: the repair scenario requires that $j(z)$ vanishes at $h = h_e$. This can be achieved by setting $h = h_e$ in (14b) and solving for c_t , yielding

$$c_t = c_s \left[\frac{\left(\sqrt{J^2 + 4\xi S_c} - J \right) e^{-\left(\frac{h_e J}{S_e} + \frac{h_i J}{S_i} + \frac{h_w J}{S_w} \right)}}{J + \sqrt{J^2 + 4\xi S_c} - 2 \sqrt{J^2 + 4\xi S_c} e^{\left(\frac{h_e J - h_c \sqrt{J^2 + 4\xi S_c}}{2S_c} \right)}} \right]_{h=h_e} \quad (25)$$

(Notice that J depends — according to (9) — also on h_e .) Insertion of this result into (14) (i) guarantees that $j(z)$ vanishes at $h = h_e$ and (ii) eliminates c_t from $j(z)$.

To make up for the lack of input data for c_s , ξ , S_c and the K_n ($i = w, i, e$) we resort to educated guesses of some parameters, guided by model immanent criteria. We proceed as follows:

Table 1: List of variables and numerical values. Subscripts c, w, i, e refer to the different structural layers depicted in Figure 1. Numerical data for diffusion constants and thicknesses of cutin layer and wax film layer are partly based on Tables 2 and 3 in [68] for cultivar “Elstar” and partly derived by educated guessing. For details see section 3.3. Similarly, the value of K_c is based on [69]. The diffusion constant of the polysaccharide layer has been set arbitrarily to one tenth of the diffusion constant of the cutin layer

Quantity	Value	Description, Sources
R	8.314 J/mol/K	gas constant
T	20 °C	temperature
g	9.81 m/s ²	gravitational acceleration
V_w	18.07×10^{-6} m ³ /mol	molar volume of liquid water
V_{wax}	404×10^{-6} m ³ /mol	molar volume of wax
ρ_w	18.07×10^{-6} m ³ /mol	density of liquid water
w_{rel}	0.6	relative atmospheric humidity
ψ_{leaf}	-204 m	leaf water potential in units of pressure head, equivalent to -2 MPa, [70]
ξ	4/s	rate constant of wax production in epidermal cell
c_s	10 mol/m ³	saturation concentration of wax molecules
c_t	5.53 mol/m ³	threshold concentration of wax molecules in epidermal cell
h_c	16 μ m	thickness of epidermal cell layer
h_w	0.5 μ m	thickness of polysaccharide layer
h_i	11.93 μ m	thickness of cutin layer
h_e	4.14 μ m	thickness of epicuticular wax film,
S_c	4.33×10^{-12} m ² /s	diffusion constant of epidermal cell layer
S_w	7.16×10^{-11} m ² /s	diffusion constant of polysaccharide layer
S_i	7.16×10^{-10} m ² /s	diffusion constant of cutin layer
S_e	3.03×10^{-10} m ² /s	diffusion constant of epicuticular wax film
K_c	1×10^{-14} m/s	hydraulic conductivity of epidermal cell layer
K_w	1.69×10^{-15} m/s	hydraulic conductivity of polysaccharide layer
K_i	1.69×10^{-14} m/s	hydraulic conductivity of cutin layer
K_e	7.18×10^{-15} m/s	hydraulic conductivity of epicuticular wax film

- Values for the diffusion constants S_n ($n = w, i, e$) are available especially for apple cultivars (see e.g.[71, 68, 72]), while the related hydraulic conductivities are not. Assuming that the K_n are roughly proportional to the S_n (as suggested in [69]),

$$K_c \approx \beta S_c \quad (26)$$

$$K_n \approx \alpha S_n \quad n = w, i, e \quad , \quad (27)$$

one finds $\alpha = 0.236 \times 10^{-4}/\text{m}$ and $\beta = 2.30 \times 10^{-3}/\text{m}$ from requiring that the arguments of the exponentials in (14b) are approximately equal to 1, in order to obtain physically reasonable results.

This conclusion is corroborated by noting that the reciprocals of these terms represent the Peclet numbers $\text{Pe} = S_e/(h_e J)$ etc.. Since the Peclet number measures whether particle transport is dominated by diffusion or advection and since our repair scenario assumes that these mechanisms are in equilibrium for an undamaged cuticle, values of $\text{Pe} \approx 1$ are to be expected.

- Furthermore, $j(z)$ ought to have a negative slope at $h = h_e$. Otherwise, the wax flux points toward the plant interior for $0 < h < h_e$. Playing around with orders of magnitudes one finds that this criterion can be met by multiplying the so far obtained values of the K_n and S_n ($n = w, i, e$) by the factor 10^4 and by dividing K_c by 10^4 (for the resulting numbers see Table 1).
- The remaining unknown ξ follows from requiring $t_{95} \approx 4$ h at $w_{rel} = 0.6$, the time it takes to repair 95 % of the thickness of the damaged film.
- The saturation value $c_s = 10 \text{ mol/m}^3$ of the wax concentration is the result of a guess which fits well into the already estimated data.

4 Conclusions

The model presented above corroborates the conjecture of Neinhuis, Koch et al. [62] who proposed the co-transport of wax components with water instead of postulating carrier molecules or specialised pathways for wax molecules and were also able to confirm their hypothesis qualitatively by carrying out experiments with isolated cuticles and artificial membranes.

The model presented here explains these findings in detail and allows quantitative predictions also for living plants, provided a complete and consistent data set of the variables used in the model is available. At the moment, however, the lack of data precludes the validation of the model.

References

- [1] T. H. Yeats and J. K. Rose. The formation and function of plant cuticles. *Plant physiology*, **163**(1), 5 (2013)
- [2] T. N. Taylor, E. L. Taylor, and M. Krings. *Paleobotany*. Academic Press, Amsterdam (2009)
- [3] J. Schönherr, F. Kerler, and M. Riederer. Cuticular lipids as interfaces between plant and environment. *Dev. Plant Biol.*, **9**, 491 (1984)

- [4] M. Riederer and L. Schreiber. *Waxes — the transport barriers of plant cuticles*, volume 6, pages 131–156. The Oily Press, Dundee, Scotland (1995)
- [5] P. Kolattukudy. *Polyesters in higher plants*, pages 4–49. Springer Verlag, Berlin (2001)
- [6] A. Heredia. Biophysical and biochemical characteristics of cutin, a plant barrier biopolymer. *Biochimica et Biophysica Acta — General Subjects*, **1620**(1-3), 1 (2003)
- [7] M. Riederer and C. Müller. *Biology of the plant cuticle*. Blackwell (2006)
- [8] J. J. Benitez, R. Garcia-Segura, and A. Heredia. Plant biopolyester cutin: a tough way to its chemical synthesis. *Biochimica Et Biophysica Acta-General Subjects*, **1674**(1), 1 (2004)
- [9] J. P. Douliez, J. Barrault, F. Jerome, A. Heredia, L. Navailles, and F. Nallet. Glycerol derivatives of cutin and suberin monomers: Synthesis and self-assembly. *Biomacromolecules*, **6**(1), 30 (2005)
- [10] C. E. Jeffree. *The fine structure of the plant cuticle*, volume 23 of *Annual Plant Reviews*. Blackwell (2006)
- [11] R. E. Stark and S. Tian. *The cutin biopolymer matrix*, volume 23 of *Annual Plant Reviews*. Blackwell (2006)
- [12] A. Heredia, J. A. Heredia-Guerrero, E. Dominguez, and J. J. Benitez. Cutin synthesis: A slippery paradigm. *Biointerphases*, **4**(1), P1 (2009)
- [13] E. Domingues, J. A. Heredia-Guerrero, and A. Heredia. The biophysical design of plant cuticles: an overview. *New Phytologist*, **189**, 938 (2011)
- [14] C. E. Jeffree. *The cuticle, epicuticular waxes and trichomes of plants, with reference to their structure, functions and evolution*, pages 23–63. Edward Arnold, London (1986)
- [15] P. Holloway. *Plant cuticles: physicochemical characteristics and biosynthesis*, pages 1–13. NATO ASI Series. Springer, Berlin (1994)
- [16] P. Kolattukudy. *Biosynthetic pathways of cutin and waxes*, pages 83–108. Environmental plant biology. Bios Scientific, Oxford (1996)
- [17] K. Espelie, B. Dean, and P. Kolattukudy. Composition of lipid-derived polymers from different anatomical regions of several plant species. *Plant Physiology*, **64**, 1089 (1979)
- [18] E. Baker, M. Bucovac, and G. Hunt. *Composition of tomato fruit cuticle as related to fruit growth and development*, pages 33–44. Academic Press, London, New York (1982)
- [19] F. Marga, T. Pesacreta, and K. Hasenstein. Biochemical analysis of elastic and rigid cuticles of *Cirsium horridulum* Michx. *Planta*, **213**, 841 (2001)
- [20] R. Stark, B. Yan, A. Ray, Z. Chen, X. Fang, and J. Garbow. NMR studies of structure and dynamics in fruit cuticle polyesters. *Solid State Nuclear Magnetic Resonance*, **16**, 37 (2000)
- [21] J. F. Villena, E. Dominguez, and A. Heredia. Monitoring biopolymers present in plant cuticles by FT-IR spectroscopy. *Journal of Plant Physiology*, **156**(3), 419 (2000)

- [22] J. J. Benitez, J. A. Heredia-Guerrero, F. M. Serrano, and A. Heredia. The Role of Hydroxyl Groups in the Self-Assembly of Long Chain Alkylhydroxyl Carboxylic Acids on Mica. *Journal of Physical Chemistry C*, **112**(43), 16968 (2008)
- [23] A. Matas and A. Heredia. Molecular dynamics modellization and simulation of water diffusion through plant cutin. *Zeitschrift für Naturforschung C*, **54**(11), 896 (1999)
- [24] C. Popp, M. Burghardt, A. Friedmann, and M. Riederer. Characterization of hydrophilic and lipophilic pathways of *Hedera helix* L. cuticular membranes: permeation of water and uncharged organic compounds. *Journal of Experimental Botany*, **56**(421), 2797 (2005)
- [25] W. Barthlott. Epidermal and seed surface characters of plants: systematic applicability and some evolutionary aspects. *Nord. J. Bot.*, **3**, 345 (1981)
- [26] W. Barthlott and I. Theisen. Epicuticular wax ultrastructure and classification of Ranunculiflorae. *Pl. Syst. Evol. (Suppl.)*, **9**, 39 (1995)
- [27] W. Barthlott, C. Neinhuis, D. Cutler, F. Ditsch, I. Meusel, I. Theisen, and H. Wilhelm. Classification and terminology of plant epicuticular waxes. *J. Linn. Soc.*, **126**, 137 (1998)
- [28] K. Conn and J. Tewari. Ultrastructure of epicuticular wax in canola. *Z. Naturforsch.*, **44c**, 705 (1989)
- [29] H. J. Ensikat, C. Neinhuis, and W. Barthlott. Direct access to plant epicuticular wax crystals by a new mechanical isolation method. *International Journal of Plant Sciences*, **161**(1), 143 (2000)
- [30] K. Koch, A. Dommissé, C. Neinhuis, and W. Barthlott. *Self-assembly of epicuticular waxes on living plant surfaces by atomic force microscopy*, pages 457–460. American Institute of Physics, Melville (NY, USA) (2003)
- [31] R. Jetter, S. Schäffer, and M. Riederer. Leaf cuticular waxes are arranged in chemically and mechanically distinct layers: evidence from *Prunus laurocerasus* L. *Plant, Cell and Environment*, **23**, 619 (2000)
- [32] O. Guhling, C. Kinzler, M. Dreyer, G. Bringmann, and R. Jetter. Surface composition of myrmecophilic plants: Cuticular wax and glandular trichomes on leaves of *Macaranga tanarius*. *Journal of Chemical Ecology*, **31**(10), 2323 (2005)
- [33] R. Jetter, L. Kunst, and A. L. Samuels. *Composition of plant cuticular waxes*, volume 23 of *Annual Plant Reviews*. Blackwell (2006)
- [34] T. Walton. *Waxes, Cutin and Suberin*, volume 4 of *Methods in Plant Biochemistry*, pages 105–158. Academic Press, London (1990)
- [35] G. Bianchi. *Plant waxes*, volume 6, pages 175–222. The Oily Press, Glasgow (1995)
- [36] E. Wollenweber, M. Doerr, K. Siems, R. Faure, I. Bombarda, and E. M. Gaydou. Triterpenoids in lipophilic leaf and stem coatings. *Biochemical Systematics and Ecology*, **27**(1), 103 (1999)
- [37] E. Wollenweber, M. Dorr, and J. N. Roitman. Epicuticular flavonoids of some Scrophulariaceae. *Zeitschrift für Naturforschung C-a Journal of Biosciences*, **55**(1-2), 5 (2000)

- [38] M. Riederer and C. Markstädter. *Cuticular waxes: a critical assessment of current knowledge*, pages 189–200. Bios Scientific, Oxford (1996)
- [39] M. Riederer and L. Schreiber. Protecting against water loss: analysis of the barrier properties of plant cuticles. *Journal of Experimental Botany*, **52**(363), 2023 (2001)
- [40] R. Jetter and M. Riederer. In vitro reconstitution of epicuticular wax crystals: Formation of tubular aggregates by long chain secondary alkanediols. *Bot. Acta*, **108**, 111 (1995)
- [41] R. Jetter and M. Riederer. Epicuticular crystals of nonacosan-10-ol: In-vitro reconstitution and factors influencing crystal habits. *Planta*, **195**, 257 (1994)
- [42] I. Meusel, W. Barthlott, H. Kutzke, and B. Barbier. Crystallographic studies of plant waxes. *Powder Diffraction*, **15**(2), 123 (2000)
- [43] A. J. Matas, M. J. Sanz, and A. Heredia. Studies on the structure of the plant wax nonacosan-10-ol, the main component of epicuticular wax conifers. *International Journal of Biological Macromolecules*, **33**(1-3), 31 (2003)
- [44] B. Baum, A. Tulloch, and L. Bailey. Epicuticular waxes of the genus *Hordeum*: a survey of their chemical composition and ultrastructure. *Canadian Journal of Botany*, **67**, 3219 (1989)
- [45] W. Barthlott, I. Theisen, T. Borsch, and C. Neinhuis. *Epicuticular waxes and vascular plant systematics: integrating micromorphological and chemical data*, volume *Regnum Vegetabile*, 141, pages 189–206. Gantner Verlag, Ruggell (2003)
- [46] N. Hallam and T. Chambers. The leaf waxes of the genus *Eucalyptus* L'Heritier. *Aust. J. Bot.*, **18**, 335 (1970)
- [47] K. Koch, W. Barthlott, S. Koch, A. Hommes, K. Wandelt, W. Mamdouh, S. De-Feyter, and P. Broekmann. Structural analysis of wheat wax (*Triticum aestivum*, c.v. 'Naturastar' L.): from the molecular level to three dimensional crystals. *Planta*, **223**(2), 258 (2005)
- [48] I. Meusel, C. Neinhuis, C. Markstadter, and W. Barthlott. Ultrastructure, chemical composition, and recrystallization of epicuticular waxes: transversely ridged rodlets. *Canadian Journal of Botany-Revue Canadienne De Botanique*, **77**(5), 706 (1999)
- [49] M. Whitecross and D. Armstrong. Environmental effects on epicuticular waxes of *Brassica napus* L. *Aust. J. Bot.*, **20**, 87 (1972)
- [50] D. Armstrong and M. Whitecross. Temperature effects on formation and fine structure of *Brassica napus* leaf waxes. *Austr. J. Bot.*, **24**, 309 (1976)
- [51] K. Koch, A. Domisse, and W. Barthlott. Chemistry and crystal growth of plant wax tubules of *Lotus (Nelumbo nucifera)* and *Nasturtium (Tropaeolum majus)* leaves on technical substrates. *Crystal Growth and Design*, **6**, 2571 (2006)
- [52] H. J. Ensikat, B. Boese, W. Mader, W. Barthlott, and K. Koch. Crystallinity of plant epicuticular waxes: electron and x-ray diffraction studies. *Chemistry and Physics of Lipids*, **144**, 45 (2006)
- [53] A. d. Bary. Über die Wachsüberzüge der Epidermis. *Botanische Zeitschrift*, **29**, 128 (1871)

- [54] L. Schreiber, K. Schorn, and T. Heimbürg. H-2 NMR study of cuticular wax isolated from *Hordeum vulgare* L. leaves: identification of amorphous and crystalline wax phases. *European Biophysics Journal with Biophysics Letters*, **26**(5), 371 (1997)
- [55] C. Jeffree, E. Baker, and P. Holloway. Ultrastructure and recrystallization of plant epicuticular waxes. *New Phytol.*, **75**, 539 (1975)
- [56] K. Koch, C. Neinhuis, H. J. Ensikat, and W. Barthlott. Self assembly of epicuticular waxes on living plant surfaces imaged by atomic force microscopy (AFM). *Journal of Experimental Botany*, **55**(397), 711 (2004)
- [57] K. Koch, A. Dommissé, A. Niemiézt, W. Barthlott, and K. Wandelt. Nanostructure of epicuticular plant waxes: Self-assembly of wax tubules. *Surface science*, **603**(10-12), 1961 (2009)
- [58] W. Franke. Ectodesmata and the cuticular penetration of leaves. *Pestic. Sci.*, **1**, 164 (1970)
- [59] L. Schreiber. Polar paths of diffusion across plant cuticles: new evidence for an old hypothesis. *Annals of Botany*, **95**(7), 1069 (2005)
- [60] L. Samuels, R. Jetter, and L. Kunst. First steps in understanding the export of lipids to the plant cuticle. *Plant Biosystems*, **139**(1), 65 (2005)
- [61] D. Canet, R. Rohr, A. Chamel, and F. Guillain. Atomic force microscopy study of isolated ivy leaf cuticles observed directly and after embedding in Epon(R). *New Phytologist*, **134**(4), 571 (1996)
- [62] C. Neinhuis, K. Koch, and W. Barthlott. Movement and regeneration of epicuticular waxes through plant cuticles. *Planta*, **213**, 427 (2001)
- [63] J. A. Heredia-Guerrero, J. J. Benitez, and A. Heredia. Self-assembled polyhydroxy fatty acids vesicles: a mechanism for plant cutin synthesis. *Bioessays*, **30**(3), 273 (2008)
- [64] P. A. Domenico and F. W. Schwartz. *Physical and chemical hydrogeology*, volume 44. Wiley New York (1998)
- [65] R. A. Freeze and J. A. Cherry. *Groundwater*. Prentice-Hall (1977)
- [66] P. S. Nobel. *Physicochemical and environmental plant physiology*. Elsevier Academic Press, Amsterdam, 3. ed. edition (2005)
- [67] F. Reif. *Fundamentals of statistical and thermal physics*. McGraw-Hill, New York (1974)
- [68] E. A. Veraverbeke, P. Verboven, N. Scheerlinck, M. L. Hoang, and B. M. Nicolai. Determination of the diffusion coefficient of tissue, cuticle, cutin and wax of apple. *Journal of Food Engineering*, **58**(3), 285 (2003)
- [69] L. Schreiber and M. Riederer. Determination of diffusion coefficients of octadecanoic acid in isolated cuticular waxes and their relationship to cuticular water permeabilities. *Plant, Cell & Environment*, **19**(9), 1075 (1996)
- [70] W. Larcher. *Physiological plant ecology: ecophysiology and stress physiology of functional groups*. Springer Science & Business Media (2003)

- [71] E. A. Veraverbeke, P. Verboven, P. V. Oostveldt, and B. M. Nicolai. Prediction of moisture loss across the cuticle of apple (*Malus sylvestris* subsp. *mitis* (Wallr.) during storage. *Postharvest Biology and Technology*, **30**(1), 75 (2003)
- [72] A. Konarska. Morphological, Histological and Ultrastructural Changes in Fruit Epidermis of Apple *Malus Domestica* cv. Ligol (Rosaceae) at Fruit Set, Maturity and Storage. *Acta Biologica Cracoviensia s. Botanica*, **56**(2) (2015)